

Downloaded from UvA-DARE, the institutional repository of the University of Amsterdam (UvA)
<http://hdl.handle.net/11245/2.30282>

File ID uvapub:30282
Filename 136557y.pdf
Version unknown

SOURCE (OR PART OF THE FOLLOWING SOURCE):

Type article
Title Exclusive production of pp-bar pi+ pi- in photon-photon collisions
Author(s) H. Aihara, M. Alston-Garnjost, R.E. Avery, A. Barbaro-Galtieri, A.R. Barker,
 B.A. Barnett, D.A. Bauer, A. Bay, F.L. Linde
Faculty UvA: Universiteitsbibliotheek
Year 1989

FULL BIBLIOGRAPHIC DETAILS:

<http://hdl.handle.net/11245/1.425942>

Copyright

It is not permitted to download or to forward/distribute the text or part of it without the consent of the author(s) and/or copyright holder(s), other than for strictly personal, individual use, unless the work is under an open content licence (like Creative Commons).

Exclusive production of $p\bar{p}\pi^+\pi^-$ in photon-photon collisions

H. Aihara,¹ M. Alston-Garnjost,^a R. E. Avery,^a A. Barbaro-Galtieri,^a A. R. Barker,^g
 B. A. Barnett,¹ D. A. Bauer,^g A. Bay,^a G. J. Bobbink,^k C. D. Buchanan,^d A. Buijs,^k
 D. O. Caldwell,^g H-Y. Chao,^h S-B. Chun,^d A. R. Clark,^a G. D. Cowan,^a D. A. Crane,ⁱ
 O. I. Dahl,^a M. Daoudi,^c K. A. Derby,^a J. J. Eastman,^a P. H. Eberhard,^a T. K. Edberg,^a
 A. M. Eisner,^c F. C. Ern ,^k K. H. Fairfield,^f J. M. Hauptman,^h W. Hofmann,^a J. Hylen,ⁱ
 T. Kamae,¹ H. S. Kaye,^a R. W. Kenney,^a S. Khacheryan,^d R. R. Kofler,^j
 W. G. J. Langeveld,^c J. G. Layter,^c W. T. Lin,^e F. L. Linde,^k S. C. Loken,^a
 G. R. Lynch,^a R. J. Madaras,^a B. D. Magnuson,^c G. E. Masek,^f L. G. Mathis,^a
 J. A. J. Matthews,ⁱ S. J. Maxfield,^j E. S. Miller,^f W. Moses,^a D. R. Nygren,^a
 P. J. Oddone,^a H. P. Paar,^f S. K. Park,^h D. E. Pellett,^b M. Pripstein,^a M. T. Ronan,^a
 R. R. Ross,^a F. R. Rouse,^a K. A. Schwitkis,^g J. C. Sens,^k G. Shapiro,^a B. C. Shen,^c
 J. R. Smith,^b J. S. Steinman,^d R. W. Stephens,^g M. L. Stevenson,^a D. H. Stork,^d
 M. G. Strauss,^d M. K. Sullivan,^c T. Takahashi,¹ S. Toutouchi,^j R. van Tyen,^a
 W. Vernon,^f W. Wagner,^b E. M. Wang,^a Y-X. Wang,^g W. A. Wenzel,^a Z. R. Wolf,^a
 H. Yamamoto,^a S. J. Yellin,^g and C. Zeitlin^b

(TPC/Two-Gamma Collaboration)

^aLawrence Berkeley Laboratory, University of California, Berkeley, California 94720

^bUniversity of California, Davis, California 95616

^cUniversity of California Intercampus Institute for Research at Particle Accelerators, Stanford, California 94305

^dUniversity of California, Los Angeles, California 90024

^eUniversity of California, Riverside, California 92521

^fUniversity of California, San Diego, California 92093

^gUniversity of California, Santa Barbara, California 93106

^hAmes Laboratory, Iowa State University, Ames, Iowa 50011

ⁱJohns Hopkins University, Baltimore, Maryland 21218

^jUniversity of Massachusetts, Amherst, Massachusetts 01003

^kNational Institute for Nuclear and High Energy Physics, Amsterdam, The Netherlands

¹University of Tokyo, Tokyo, Japan

(Received 7 April 1989)

We report a measurement of the $e^+e^- \rightarrow e^+e^-p\bar{p}\pi^+\pi^-$ process with the TPC/Two-Gamma facility at the PEP e^+e^- storage ring at SLAC. Forty-five $p\bar{p}\pi^+\pi^-$ events were identified in data corresponding to an integrated e^+e^- luminosity of 142 pb^{-1} . The cross section for $\gamma\gamma \rightarrow p\bar{p}\pi^+\pi^-$ is given both as a function of the $\gamma\gamma$ center-of-mass energy $W_{\gamma\gamma}$, with $W_{\gamma\gamma}$ between 2.5 and 5.5 GeV, and as a function of the invariant mass squared q^2 of one of the photons, with $-q^2 < 7 \text{ GeV}^2$. This cross section falls much less rapidly with $W_{\gamma\gamma}$ than does the cross section for a similar process, $\gamma\gamma \rightarrow p\bar{p}$. No $\Delta^0\bar{\Delta}^0$ production is observed, and only a small fraction of the events at low $W_{\gamma\gamma}$ is consistent with $\gamma\gamma \rightarrow \Delta^{++}\bar{\Delta}^{--}$, $\Delta^{++}\bar{p}\pi^-$, or $\bar{\Delta}^{--}p\pi^+$. In an expanded search through the same data, four events compatible with either $\Lambda\bar{\Lambda}$ ($\Lambda \rightarrow p\pi^-$) or $\Sigma^0\bar{\Lambda}$ ($\Sigma^0 \rightarrow \Lambda\gamma$) production were found.

The exclusive production of meson and baryon pairs in photon-photon collisions has been considered to be a testing ground for perturbative QCD by several authors.¹⁻³ These QCD calculations predict a power-law behavior as a function of the $\gamma\gamma$ center-of-mass energy $W_{\gamma\gamma}$. For baryon pairs this leads to a $W_{\gamma\gamma}^{-10}$ dependence of the cross section at a fixed center-of-mass angle at large values of the momentum transfer squared ($|t| > 5 \text{ GeV}^2$). A $W_{\gamma\gamma}$ dependence compatible with this prediction was indeed observed⁴ for the cross section of $\gamma\gamma \rightarrow p\bar{p}$, at lower values of $|t|$. However the values for the $\gamma\gamma \rightarrow p\bar{p}$ cross section in the invariant-mass range between 2.4 and 2.8

GeV derived by the TASSO,⁵ JADE,⁶ and TPC/Two-Gamma⁴ Collaborations are about an order of magnitude higher than the predicted values. Production of some other baryon pairs, $\Delta^{++}\bar{\Delta}^{--}$, $\Delta^0\bar{\Delta}^0$, and $\Lambda\bar{\Lambda}$, can be studied via the $\gamma\gamma \rightarrow p\bar{p}\pi^+\pi^-$ process. A first observation of 15 events from the reaction $\gamma\gamma \rightarrow p\bar{p}\pi^+\pi^-$ was reported by the TASSO Collaboration;⁷ no significant $\Delta^{++}\bar{\Delta}^{--}$, $\Delta^0\bar{\Delta}^0$, or $\Lambda\bar{\Lambda}$ signals were observed, and upper limits for cross sections were given.

We report here a measurement of the reaction $e^+e^- \rightarrow e^+e^-p\bar{p}\pi^+\pi^-$ with the TPC/Two-Gamma facility⁸ at the PEP e^+e^- storage ring at SLAC, with in-

cident e^+ and e^- energies of 14.5 GeV. The data were collected in two periods. In the first, the time-projection chamber (TPC) was operated in a 0.389-T magnetic field, providing a momentum resolution of $(\delta p/p)^2 = (0.06)^2 + (0.035p)^2$ (p in GeV) for charged particles at large angles with respect to the beam axis. In the second period, the TPC was operated in a 1.325-T magnetic field from a superconducting solenoid, with a momentum resolution of $(\delta p/p)^2 = (0.015)^2 + (0.0065p)^2$ (p in GeV). The TPC also sampled energy loss (dE/dx) along particle trajectories, with a typical resolution of 3.6%. This was used for hadron identification. Two proportional-mode pole-tip calorimeters (PTC) and a hexagonal Geiger-mode calorimeter (HEX) covered polar angles above 260 mrad. In a fraction of the events either the scattered electron or positron (a ‘‘tag’’) was detected in one of two arrays of NaI crystals in the angular range 25–90 mrad or lead-scintillator shower counters from 100 to 180 mrad, and in one of two arrays of 15 drift-chamber planes in front of these detectors. The NaI and shower-counter energy resolutions at 14.5 GeV were 1.5% and 5% rms, respectively.

Our untagged trigger, based on information in the central detector, required at least two charged tracks in the TPC, each with polar angle $\theta \gtrsim 26^\circ$ and projecting back to the interaction point within 20 cm along the beam axis. Tracks with $\theta > 45^\circ$ were required to be in coincidence with hits in a drift chamber (ODC) outside the coil of the solenoid. Our single-tag trigger required one TPC track with $\theta \gtrsim 26^\circ$ in coincidence with an energy deposition in either tagging calorimeter. The untagged (tagged) data selected correspond to an integrated luminosity of 73 (50) and 69 (67) pb^{-1} for the two data-taking periods, respectively.

In this four-prong analysis we selected events with two positively and two negatively charged tracks coming from the interaction point. Two tracks were required to have $\theta > 30^\circ$ (20°) for the untagged (tagged) data. Minimum momenta of 0.1, 0.3, and 0.4 GeV were required for pions, kaons, and (anti)protons, respectively. For tagged events the scattered leptons were required to have $E > 6$ GeV and reconstructed tracks in the forward drift chambers. For particle identification we used an algorithm which compares the measured dE/dx (defined as the average of the lowest 65% of the samples) and the momentum to empirically determined curves for the various particle types (e, μ, π, K, p) and determines a χ^2 for each type. From these a confidence level was calculated for $p\bar{p}\pi^+\pi^-$, and for a number of final states that could be confused with it: $\pi^+\pi^-\pi^+\pi^-$, $K^+K^-K^+K^-$, $K^+K^-\pi^+\pi^-$, $K^\pm\pi^\mp K_S^0$ ($K_S^0 \rightarrow \pi^+\pi^-$), $e^+e^-e^+e^-$, $p\bar{p}\gamma$ ($\gamma \rightarrow e^+e^-$), and $K^+K^-\gamma$ ($\gamma \rightarrow e^+e^-$). We required a confidence level in excess of 10% for $p\bar{p}\pi^+\pi^-$. This confidence level also had to be larger than that of other final states. In addition, we required the confidence level for the frequently occurring $\pi^+\pi^-\pi^+\pi^-$ state to be less than 1%. Figure 1(a) shows the distribution of the measured dE/dx versus momentum for all four particles in the accepted events. Clearly visible is the separation between pions and protons.

All event candidates were scanned by eye for possible

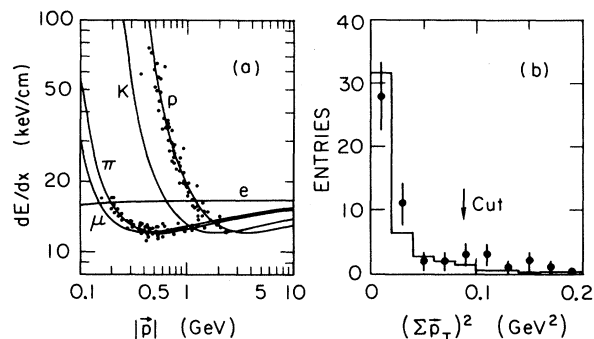


FIG. 1. (a) Distribution of the mean energy loss vs momentum, as measured by the TPC, for particles in the selected $p\bar{p}\pi^+\pi^-$ sample. The solid lines represent the curves for the various particle types. (b) The square of the vector sum of the transverse particle momenta for the selected $p\bar{p}\pi^+\pi^-$ sample. The sum includes the tagging electron if present. The histogram indicates the Monte Carlo simulation of the process.

extra tracks which were not reconstructed as coming from the vertex. If there appeared to be an additional, but scattered, track from the vertex, the event was rejected. Events where one of the four tracks backscattered from the surrounding detectors were kept. Events with extra energy depositions above 150 MeV in the HEX or 250 MeV in the PTC were rejected if no correlation with tracks from charged particles was found. The summed transverse momentum of the four charged particles and possible tags, p_T , was required to be less than 0.3 GeV. In the total data sample we identified 45 $p\bar{p}\pi^+\pi^-$ events, of which 10 were tagged. No events from this sample were compatible with the possible background final state $e^-\pi^+\pi^-\pi^-$ from beam-gas collisions. In a search for $\Lambda\bar{\Lambda}$ candidates with $\Lambda \rightarrow p\pi^-$, the vertex requirements on the tracks were relaxed and extra photons were permitted, so as to include possible $\Sigma^0 \rightarrow \Lambda\gamma$ decays. We found four $p\bar{p}\pi^+\pi^-$ candidates with both $p\pi^-$ and $\bar{p}\pi^+$ pair masses within 30 MeV of the Λ mass with $p_T < 0.3$ GeV. We checked that the decay vertex distribution was compatible with the Λ lifetime. These events were treated separately from the continuum sample.

To determine the acceptance, Monte Carlo events were generated according to the luminosity function for transversely polarized photons,⁹ using an isotropic phase-space model for $\gamma\gamma \rightarrow p\bar{p}\pi^+\pi^-$. The events were processed through a detector simulation (which included resolution effects, energy loss, multiple scattering, and nuclear interactions in the detector materials), and then passed through the same cuts as the data. The selection and reconstruction efficiency averaged around 3% for a $W_{\gamma\gamma}$ of 2.5 GeV and increased to around 8% for a $W_{\gamma\gamma}$ of 5.5 GeV. The trigger efficiency was determined by simulating the trigger requirements in detail; it increased from 50% to 80% over the same $W_{\gamma\gamma}$ range.

We compared various event characteristics simulated by the Monte Carlo program with those of the selected event sample. There was satisfactory agreement for the distribution of vertices along the beam direction, the

summed longitudinal and transverse momenta of the four hadrons and the energies of the tagging electrons. In Fig. 1(b) we show a distribution of the square of the sum of the transverse particle momenta. Here the sum includes the tagging electron if present. The distribution is sharply peaked at zero as expected from the Monte Carlo calculation, which is also indicated, thus verifying the exclusive nature of the selected events. From the slightly flatter distribution of the data, we conclude that a small fraction, estimated to be $(11 \pm 4)\%$, originates from multiprong final states of which only four charged particles were detected.

In Figs. 2(a)–2(d) we show the invariant-pair-mass distributions for $p\pi^-$ ($\bar{p}\pi^+$), $p\pi^+$ ($\bar{p}\pi^-$), $\pi^+\pi^-$, and $p\bar{p}$, together with Monte Carlo-generated distributions from isotropic $p\bar{p}\pi^+\pi^-$ phase space, in which the Monte Carlo distribution in $W_{\gamma\gamma}$ is made to follow the experimental one. The distributions in the cosine of the angle $\theta_{p\pi^+}^*$ defined by the $p\pi^+$ direction in the $\gamma\gamma$ center-of-mass system, and the cosine of the angle θ_p of the proton with respect to the photon direction in the $p\pi^+$ center-of-mass system (Adair frame) are shown in Figs. 3(a) and 3(b) along with Monte Carlo predictions based upon the same phase-space model. One observes that this simple model gives a satisfactory description of the pair mass and angular distributions. In particular, the low-mass enhancements in the $p\pi$ pair distributions need at most a small contribution from $\Delta\bar{\Delta}$ ($M_\Delta=1.232$ GeV, $\Gamma_\Delta=0.115$ GeV). We note that the effective mass resolution is on the average 10 MeV at the Δ mass, much smaller than the Δ width. In Figs. 4(a) and 4(b) we show scatter plots of the $p\pi$ mass combinations. There is little clustering in the $\Delta\bar{\Delta}$ mass range.

The fractions of the phase space $\Delta^{++}\bar{\Delta}^{--}$ and $\Delta^0\bar{\Delta}^0$ contributions in the $p\bar{p}\pi^+\pi^-$ event sample are deter-

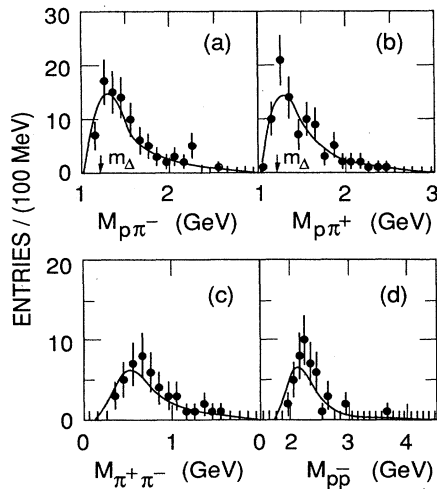


FIG. 2. Effective pair-mass distributions (a) of $p\pi^-$ and $\bar{p}\pi^+$, (b) of $p\pi^+$ and $\bar{p}\pi^-$, (c) of $\pi^+\pi^-$, and (d) of $p\bar{p}$. The curves indicate the Monte Carlo simulation for isotropic phase space discussed in the text.

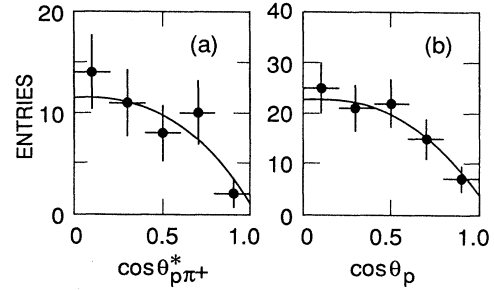


FIG. 3. Distributions of the cosines (a) of the angle $\theta_{p\pi^+}^*$ of the $p\pi^+$ system in the overall $\gamma\gamma$ c.m., (b) of the angle θ_p of the proton in the $p\pi^+$ c.m. frame. The curves indicate the Monte Carlo simulation discussed in the text.

mined by a maximum-likelihood fit after Monte Carlo generation of samples of these processes. The method has been extensively described for the determination of $\rho^0\rho^0$ and $\rho^0\pi^+\pi^-$ contributions^{10,11} to the $\gamma\gamma \rightarrow \pi^+\pi^-\pi^+\pi^-$ process. The fitted fractions are given in Table I. The results indicate a possible contribution from $\Delta^{++}\bar{\Delta}^{--}$ in the lowest $W_{\gamma\gamma}$ bin. Over the whole sample, the event fractions 0.10 ± 0.12 and 0.00 ± 0.12 are calculated for $\Delta^{++}\bar{\Delta}^{--}$ and $\Delta^0\bar{\Delta}^0$, respectively. These numbers change to 0.03 ± 0.14 and 0.00 ± 0.08 , respectively, if forward peaking is introduced in the $\Delta\bar{\Delta}$ distributions, as is expected in the QCD models from Ref. 3. Taking the $\Delta\bar{\Delta}$ fractions to be zero, we derive by a similar procedure the average fractions of single Δ production to be 0.21 ± 0.17 for $\Delta^{++}\bar{p}\pi^-$ ($\bar{\Delta}^{--}p\pi^+$) and 0.12 ± 0.15 for $\Delta^0\bar{p}\pi^+$ ($\bar{\Delta}^0p\pi^-$). Finally, Fig. 2(c) shows that there is no significant contribution from ρ^0 in the $\pi^+\pi^-$ pair mass spectrum. A fit gives an average $p\bar{p}\rho^0$ fraction of 0.01 ± 0.12 .

The untagged $\gamma\gamma \rightarrow p\bar{p}\pi^+\pi^-$ cross section, shown in Table I, is obtained after subtraction of the estimated multiprong background; it is in satisfactory agreement with the result of Ref. 7. The errors indicated are statistical only. Systematic errors include contributions from uncertainties in luminosity (5%), detector response and

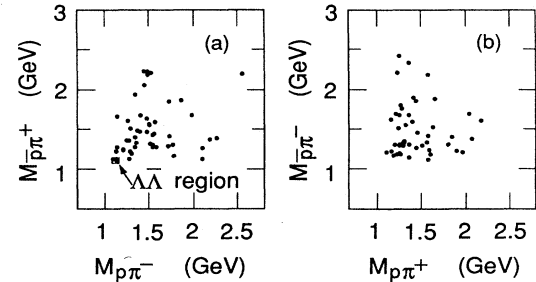


FIG. 4. Scatter plots of (a) the $\bar{p}\pi^+$ invariant mass vs the $p\pi^-$ mass, with the entries from the separate sample of four $\Lambda\bar{\Lambda}$ candidates also shown and (b) the $\bar{p}\pi^-$ invariant mass vs the $p\pi^+$ mass.

TABLE I. Cross sections and fractions of observed events attributed to $\Delta^{++}\bar{\Delta}^{--}$, $\Delta^0\bar{\Delta}^0$, and phase space (PS). The errors are statistical.

$W_{\gamma\gamma}$ (GeV)	$\sigma(\gamma\gamma \rightarrow p\bar{p}\pi^+\pi^-)$ (nb)	$\Delta^{++}\bar{\Delta}^{--}$	$\Delta^0\bar{\Delta}^0$	PS
2.5–3.0	1.9 ± 0.8	0.5 ± 0.4	0.0 ± 0.2	0.5 ± 0.4
3.0–3.5	1.7 ± 0.5	0.1 ± 0.2	0.1 ± 0.3	0.8 ± 0.3
3.5–4.0	1.1 ± 0.4	0.0 ± 0.2	0.0 ± 0.2	1.0 ± 0.2
4.0–4.5	0.6 ± 0.3	0.2 ± 0.4	0.0 ± 0.2	0.8 ± 0.4
4.5–5.5	0.07 ± 0.10	0.0 ± 0.7	0.0 ± 0.7	1.0 ± 0.7
Total		0.10 ± 0.12	0.00 ± 0.12	0.90 ± 0.15

triggering efficiency (15%), and event selection (15%), leading to an overall systematic error of 25%. In Fig. 5(a) the $\gamma\gamma \rightarrow p\bar{p}\pi^+\pi^-$ cross section is shown as a function of $W_{\gamma\gamma}$ (Ref. 12). It decreases much less steeply with $W_{\gamma\gamma}$ than does the $\gamma\gamma \rightarrow p\bar{p}$ cross section⁴ which is also shown.

Predictions for the s dependence of hard-scattering processes have been stated in the form of dimensional-counting rules.¹³ These imply that $d\sigma/dt \propto s^{2-n}f(t/s)$, where n is the number of elementary quanta participating in the initial and final states. For two-photon production of baryon pairs at fixed and large θ^* , and large $W_{\gamma\gamma}$, this leads to $d\sigma/d\cos\theta^* \propto W_{\gamma\gamma}^{-10}$. Here θ^* defines the baryon direction in the $\gamma\gamma$ center-of-mass system; it corresponds to $\theta_{p\pi^+}^*$ for the case of $\Delta^{++}\bar{\Delta}^{--}$ production. If we fit the data of Fig. 5(a) with a power-law form including a threshold factor,⁴ $\sigma(W_{\gamma\gamma}) = aW_{\gamma\gamma}^{-b}[1 - 4(m_p + m_\pi)^2/W_{\gamma\gamma}^2]^{1/2}$, with a and b free parameters, we obtain $b = 5.0 \pm 0.8$. Our earlier conclusion that the $p\bar{p}\pi^+\pi^-$ spectrum is dominated by contributions other than $\Delta\bar{\Delta}$ is consistent with this lack of agreement with the dimensional-counting rules. We found similar values of b in other four-prong processes:¹⁴ $b = 5.2 \pm 0.5$ for $\gamma\gamma \rightarrow \pi^+\pi^-\pi^+\pi^-$ and $b = 4.6 \pm 1.9$ for $\gamma\gamma \rightarrow K^+K^-\pi^+\pi^-$. This can be contrasted with the results of a similar fit for the process $\gamma\gamma \rightarrow p\bar{p}$ which yielded a

value $b = 13.2 \pm 2.3$ (Ref. 4), in agreement with the expectation from counting rules, $b = 10$.

As mentioned, we found four $p\bar{p}\pi^+\pi^-$ events which can be ascribed to the $\Lambda\bar{\Lambda}$ state. Three of the four events have a photon candidate. In two of these, the invariant $\Lambda\gamma$ or $\bar{\Lambda}\gamma$ mass is compatible with the Σ^0 mass, indicating a possible $\Sigma^0 \rightarrow \Lambda\gamma$ decay. The $\Lambda\bar{\Lambda}$ masses range from 2.8 to 3.1 GeV. This is compatible with an expected $W_{\gamma\gamma}^{-10}$ dependence of the cross section, which limits (for our integrated luminosity) the observation of $\Lambda\bar{\Lambda}$ events to masses close to threshold. A cross-section estimate in the above mass range gives $\sigma(\gamma\gamma \rightarrow \Lambda\bar{\Lambda} + \Sigma^0\bar{\Sigma}^0 + \Lambda\bar{\Sigma}^0 + \bar{\Lambda}\Sigma^0) = (1.0 \pm 0.6 \pm 0.5)$ nb. The second error is systematic; it takes into account the mass uncertainty from the possible Σ^0 origin and uncertainties in the acceptance and trigger.

Specific predictions based on QCD models have been made by Farrar *et al.*³ for numerous $\gamma\gamma \rightarrow B\bar{B}$ (B = baryon) cross sections. The marginal signal for $\Delta^{++}\bar{\Delta}^{--}$ and the absence of $\Delta^0\bar{\Delta}^0$ production are compatible with their predictions, though the current measurements are not accurate enough to test the calculations. However, for the sum $\gamma\gamma \rightarrow \Lambda\bar{\Lambda} + \Sigma^0\bar{\Sigma}^0 + \Lambda\bar{\Sigma}^0 + \bar{\Lambda}\Sigma^0$ the cross-section predictions, which depend sensitively on the baryon wave functions, are 1 or 2 orders of magnitude smaller than our value. A similar conclusion has been drawn for the $\gamma\gamma \rightarrow p\bar{p}$ process.⁴ It should be noted that the present measurements are at such low values of $W_{\gamma\gamma}$ that predictions based on QCD models may not even be applicable.

The $\gamma\gamma \rightarrow p\bar{p}\pi^+\pi^-$ cross section in the $W_{\gamma\gamma}$ range 2.5–4.0 GeV is shown in Fig. 5(b) as a function of $Q^2 = -q^2$, where q is the tagged photon four-momentum. Also shown are the parametrizations of the form $1/(1+Q^2/m^2)^2$ for $m = m_\rho$ and the value from the best fit, $m = 2.5_{-1.2}^{+\infty}$ GeV. The dependence on Q^2 appears to be flatter than it would be with a ρ -pole description.¹⁵

Summarizing, we identified 45 events of the $\gamma\gamma \rightarrow p\bar{p}\pi^+\pi^-$ reaction and determined that at most a small fraction is compatible with $\Delta^{++}\bar{\Delta}^{--}$ production at the lowest energy, $W_{\gamma\gamma} = 2.75$ GeV. The $\gamma\gamma \rightarrow p\bar{p}\pi^+\pi^-$ cross section has a $W_{\gamma\gamma}$ dependence similar to that of other four-prong channels and not nearly as steep as expected in QCD models of baryon pair production. In an extended search we found four events with a $\Lambda\bar{\Lambda}$ pair ($\Lambda \rightarrow p\pi^-$, $\bar{\Lambda} \rightarrow \bar{p}\pi^+$) in the final state. In the latter sample the presence of photons may indicate a pos-

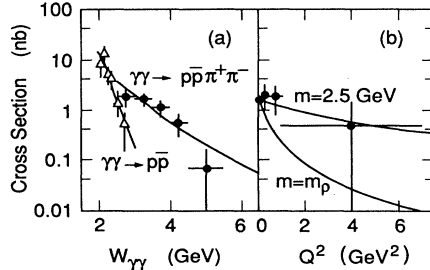


FIG. 5. (a) The cross section as a function of $W_{\gamma\gamma}$ for the processes $\gamma\gamma \rightarrow p\bar{p}\pi^+\pi^-$ and $\gamma\gamma \rightarrow p\bar{p}$. The error bars are statistical only. The $p\bar{p}$ cross section is as measured previously in our experiment (Ref. 4) for events with $|\cos\theta^*| < 0.6$. The lines indicate power-law fits as described in the text. (b) The $\gamma\gamma \rightarrow p\bar{p}\pi^+\pi^-$ cross section as a function of Q^2 for $W_{\gamma\gamma}$ between 2.5 and 4 GeV. The curves indicate a Q^2 dependence as $1/(1+Q^2/m^2)^2$ with masses m as indicated.

sible $\Sigma^0 \rightarrow \Lambda \gamma$ decay. This yield of strange-baryon pairs is substantially larger than expected from QCD models.

We thank the PEP staff for their dedication and productive running of the machine, and our engineers and technicians for their efforts in the construction and

maintenance of the detector. This work was supported in part by the United States Department of Energy, the National Science Foundation, the Joint Japan–United States Collaboration in High Energy Physics, and the Foundation for Fundamental Research on Matter in the Netherlands.

¹S. J. Brodsky and G. P. Lepage, Phys. Rev. D **24**, 1808 (1981).

²P. H. Damgaard, Nucl. Phys. **B211**, 435 (1983).

³G. R. Farrar, Phys. Rev. Lett. **53**, 28 (1984); **53**, 742(E) (1984); G. R. Farrar, E. Maina, and F. Neri, Nucl. Phys. **B259**, 702 (1985); **B263**, 746(E) (1986); G. R. Farrar, H. Zhang, A. A. Ogloblin, and I. R. Zhitnitsky, *ibid.* **B311**, 585 (1989).

⁴H. Aihara *et al.*, Phys. Rev. D **36**, 3506 (1987).

⁵M. Althoff *et al.*, Phys. Lett. **130B**, 449 (1983).

⁶W. Bartel *et al.*, Phys. Lett. B **174**, 350 (1986); **178**, 457(E) (1986).

⁷M. Althoff *et al.*, Phys. Lett. **142B**, 135 (1984).

⁸H. Aihara *et al.*, Report No. LBL-23737, 1988 (unpublished).
H. Aihara *et al.*, IEEE Trans. Nucl. Sci. **NS30**, 63 (1983); **NS30**, 67 (1983); **NS30**, 76 (1983); **NS30**, 117 (1983); **NS30**, 153 (1983); **NS30**, 162 (1983); M. P. Cain *et al.*, Phys. Lett. **147B**, 232 (1984).

⁹V. M. Budnev *et al.*, Phys. Rep. **15C**, 181 (1975).

¹⁰M. Althoff *et al.*, Z. Phys. C **16**, 13 (1982).

¹¹H. Aihara *et al.*, Phys. Rev. D **37**, 28 (1988).

¹²Other processes such as baryon pair production, $p\bar{p}\rho^0$ production, or $c\bar{c}$ bound-state production have a somewhat different $W_{\gamma\gamma}$ acceptance than the $p\bar{p}\pi^+\pi^-$ phase-space model which has been used to extract the cross section. However, we have shown that the contribution from baryon pairs and $p\bar{p}\rho^0$ in our continuum data sample is small. Monte Carlo calculations, using known branching ratios (or upper limits) and two-photon widths for the $c\bar{c}$ bound states η_c , χ_{0c} , and χ_{2c} , suggest that this contribution to the $p\bar{p}\pi^+\pi^-$ sample is also small [(10±6)%]. Thus, the effect of these other processes on the $W_{\gamma\gamma}$ dependence of the cross section is negligible to present accuracy.

¹³S. J. Brodsky and G. R. Farrar, Phys. Rev. Lett. **31**, 1153 (1973).

¹⁴A. Buijs, thesis, University of Utrecht, 1987 (unpublished).

¹⁵We note that even with a ρ -pole form factor for transverse photons, contributions from longitudinal virtual photons tend to make the Q^2 distribution somewhat flatter than the curve displayed for $m = m_\rho$.